[EN-I-012] Dynamic En-route Diversion Approach under Convective Weather

(EIWAC 2017)

+Ying Peng*, Xiangning Dong*, Xin Jiang**, and Bin Jiang*

*College of Civil Aviation, Nanjing University of Aeronautics and Astronautics
29 Jiangjun-Road, Nanjing 211106, China
joycc52@163.com

**The 709th Research Institute,China Shipbuilding Industry Corporation
No.1 north Canglong Road, Wuhan, 430200, China
1162272977@qq.com

Abstract: This paper develops a dynamic en-route diversion model for use in airspace affected by convective weather conditions. Constraints such as pilot workload and aircraft performance are considered. Based on the required level of safety for the diversion route and a single flight, a mathematical model for strategic diversion route planning is built using a genetic-annealing algorithm. The algorithm is then extended by taking into account the spatio-temporal moving characteristics of convective weather, to develop a collision model and a dynamic diversion route planning algorithm.

Keywords: dynamic enroute diversion, convective weather, route planning, genetic-annealing algorithm.

1. INTRODUCTION

With the rapid development of air transportation, delays are increasingly becoming severe. Bad weather is one of the major factors that threaten aircraft safety and cause delay. If used properly, diversion has the potential to facilitate better use of the airspace resource in order to avoid unnecessary ground holding and effectively reduce delays due to bad weather.

Research on diversion began in 1993. After two decades, some achievements have been made. In 1993, Dixon and Weidner[1] proposed a diversion strategy for the grid diversion scenario. In 2002, Song Ke[2] explored the A* search algorithm based on existing airway points. In 2009, Xu Xiaohao[3] et al. proposed a diversion route planning method based on APFA, In 2011, Maritin O.Nicholes[4] investigated a collaborative diversion route planning. In 2012, Christine Taylor and Craig Wanke[5] used a simulated annealing algorithm to plan diversion routes based on operability. In 2014, Paul F. Borchers[6] evaluated operational of a weather-avoidance rerouting system. In 2016, Chenfeng Xiong[7] et al. built an agent-based en-route diversion model.

Nowadays in-depth research on the safety of diversion routes is lacking. Our main contribution to the literature is the consideration of safety in the evolution of the storms as well as the employment of 4D trajectory capabilities. We investigates the indicators for the safety of diversion routes to enable the planning of safe and operable flight diversion routes.

2. SAFETY INDICATORS FOR DIVERSION ROUTES

When bad weather affects the planned route of an aircraft, a safe and economical diversion route should be determined. Due to minor deviations or uncertainty in the trajectory of a flight, the diversion route should be determined to keep a specified distance from the area affected by bad weather to ensure a high level of safety of a flight. Enroute safety width is set to D_R, the red area represent the weather avoid field as showed in Fig.1.

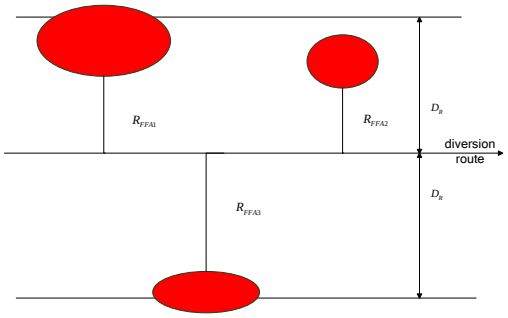

Figure 1 Weather avoid fields

For a given diversion route, and considering the volume of airspace bounded by the separation of D_R,

compute the distance between the route and every affected area, determine the minimum distance and divide by D_R to compute the safety indicator.

$$R_s = \frac{\min(R_{FFA1}, \cdots, R_{FFAi})}{D_R} \quad (1)$$

In (1), R_s denotes the safety indicator of the diversion route, D_R is the safety lateral seperation of the diversion route, R_{FFAi} is the minimum distance from the *i*th weather avoid field FFA_i to the diversion route. From (1), the variation [0,1] of the safety indicator of the diversion route can be determined. If the safe width limitation of the diversion route is not violated by the weather avoid field, then the safety indicator is 1. Moreover, if the indicator approaches 1, and the bad weather area is small, then the flight is safer. On the other hand, if the safety indicator of the diversion route approaches 0, and the blockage area is large, then the flight is more dangerous.For an instance, in Fig.2, then the safety indicator is R_{FFAi} / D_R ..

3. DIVERSION ROUTE PLANNING

Based on the safety indicator concept of the diversion route, a mathematical model for diversion route planning is developed taking into account pilot workload and aircraft performance. Genetic-annealing algorithm is adopted to find a solution to determine the global optimum of the diversion route and therefore, preventing local undesirable situations.

To alleviate the complexity of computing process, we assume that: (1) the diversion of aircraft is simplified as a process a mass point and is moving in a horizontal space; (2) weather avoid fields are represented as convex polygons; (3) aircraft flies at a constant cruising speed.

Parameter definitions are listed in table 1.

3.1 Static diversion route planning model

The precondition of realizing a static diversion route plan is to know the position and dimension of the weather avoid field during diversion. In 2009, Li Xiong[8] proposed a model to estimate the end time of diversion based on the position of the start and end points, and start time of the diversion.

$$t_d = t_s + \frac{(1+\sigma_R)D}{V_c} \quad (2)$$

t_s denotes for the start time of the diversion, t_d the ending time, σ_R the estimated percentage of the increase in the length of the route over the original route (in most cases about 20 percent); D is the original route length between the start and end points of the diversion; and V_c is the cruising speed.

Table 1 Parameter definition

Symbol	Definition
C_L	Indicator after normalization processing
C_S	Safety indicator
C_T	Number of turning point
C_A	Indicator after normalization processing of mean angle of turn of diversion route
ω_L	Weight coefficient of distance cost
ω_S	Weight coefficient of safety cost
ω_T	Weight coefficient of numbers of turning points
ω_A	Weight coefficient of turning angle changing cost
p_S	Diversion start point
p_D	Diversion end point
p_i	Turning points during diversion
$d(p_S, p_D)$	Distance between diversion start point and end point (original route length)
$d(p_i, p_{i+1})$	Distance between the two turning points during diversion
R_S^i	Safety indication of i th segment of the diversion route
N_T	Number of turning points in the diversion route
θ_i	i th turning angle in diversion route
FFA_j	j th weather avoid field during diversion
$R_S^{\min}$	Minimum safety indicator allowed in diversion route

After locating the start and end points of the diversion, the diversion end time t_d can be calculated from (2). The location and boundary of a single weather avoid field during the diversion period can be computed based on t_s、t_d. Combining all the areas during the diversion period results in the location of the whole weather avoid field.

Diversion route planning can be executed based on the location and dimension of the weather avoid field during diversion. In order to ensure that the planning results in a safe and operable diversion the optimizing model objectives are the shortest and safest diversion route, with minimum turning points and heading angle

changes. A dimensionless method is used represent each objective in order to achieve comprehensive processing of multi-objectives. Linear weights are used to transform the multiple objectives into a single objective function. The optimized diversion route is established when the minimum value of the objective function is satisfied. Hence, the planning model for diversion route is as followed:

Objective function

$$\min C = \omega_L C_L + \omega_S C_S + \omega_T C_T + \omega_A C_A \tag{3}$$

Whereby,

$$C_L = 1 - \frac{d(p_S, p_D)}{d(p_S, p_1) + \sum_{i=1}^{N_T - 1} d(p_i, p_{i+1}) + d(p_{N_T}, p_D)} \tag{4}$$

$$C_S = \frac{\sum_{i=0}^{N_T} (1 - R_S^i)}{N_T + 1} \tag{5}$$

$$C_T = \frac{N_T}{N_{\max}} \tag{6}$$

$$C_A = \frac{\sum_{i=1}^{N_T} \sin\theta_i}{N_T} \tag{7}$$

Objective function (3) represents the objective function after linear weighting. Expressions (4)~(7) represent the indicator after dimensionless processing for the length, safety of diversion route, number of tuning points and change of turning angle respectively. Every indicator could change within the range $[0,1]$, with the guarantee of the following: the less the C_L, the shorter the length of the diversion route; the less the C_S, the safer the diversion route; the less the C_T, the less the number of turning points; the less the C_A, the less the number of angle changes. The safety indicator of the diversion route R_S^i can then be determined from (1).

Restraint conditions:

$$\omega_L + \omega_S + \omega_T + \omega_A = 1 \tag{8}$$

$$\omega_L \geq 0、\ \omega_S \geq 0、\ \omega_T \geq 0、\ \omega_A \geq 0 \tag{9}$$

$$(p_i, p_{i+1}) \cap FFA_j = \varnothing \quad \forall i = 1, \ldots, N_T,\ j = 1, \ldots, n \tag{10}$$

$$d(p_i, p_{i+1}) \geq 7.4km \quad \forall i = 1, \ldots\ldots, N_T \tag{11}$$

$$\theta_i < 90° \quad \forall i = 1, \ldots\ldots, N_T \tag{12}$$

$$N_T \leq N_{\max} \tag{13}$$

$$R_S^i \geq R_S^{\min} \tag{14}$$

The restraint conditions (8) and (9) mean that the sum of all weight coefficients should be 1, each should be positive; expression (10) means the diversion route must not cross a weather avoid field; expression (11) indicates that in order to carry out the two turnings, the length of the segment should not be less than 7.4km; expression (12) indicates the highest change in turning angle should not be more than 90 degrees for the sake of safety and maneuverability; expression (13) requires that the number of diversion points should be kept to a minimum in order to reduce the workload of air traffic controllers and pilots; expression (14) requires that the safety of the diversion route should not be worse than the minimum allowable safety probability.

3.2 Dynamic diversion route planning model

A dynamic diversion route planning is executed based on the static diversion route planning, with the consideration of the direction of movement and speed of an aircraft and the weather avoid field.

3.1.1 Collision model

Assume that the following are known:

P_R: the current position of aircraft R.

θ_R: direction of aircraft movement.

V_R: aircraft speed.

P_{FFA_i}: the current position of the *i*th weather avoid field FFA_i.

θ_{FFA_i}: direction of movement of weather avoid field.

V_{FFA_i}: move speed of weather avoid field.

C_i: potential collision point of aircraft and the *i*th weather avoid field.

$D_R^{C_i}$: the distance between the aircraft and the C_i.

$\theta_R^{FFA_i}$: the angle between the planned route and the *i*th weather avoid field, $0° \leq \theta_R^{FFA_i} \leq 180°$.

$D_{FFA_i}^{C_i}$: the distance between the *i*th weather avoid field and collision point C_i.

Look upon the aircraft as a mass point. The collision is demonstrated in Figure 2. The circle represents the weather avoid field.

The collision model is set as follows:

$$V_{\max}^R = \frac{(D_R^{C_i} + r_{FFA_i}) \times V_{FFA_i}}{D_{FFA_i}^{C_i} - r_{FFA_i} - D_{route}} \tag{15}$$

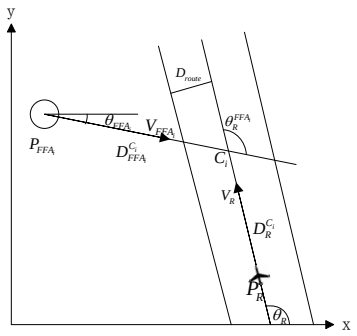

(a) Original position

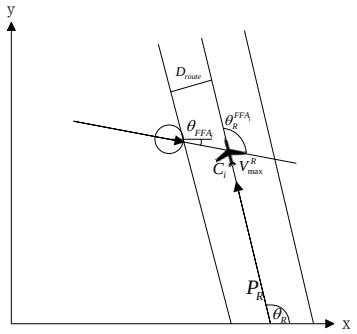

(b) no collision with $V_{\max}^R$

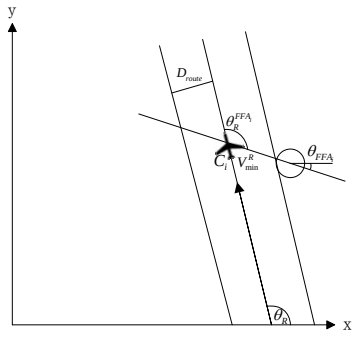

(c) no collision with $V_{\min}^R$

Figure 2 Demonstration of collision

$$V_{\min}^R = \frac{(D_R^{C_i} - r_{FFA_i}) \times V_{FFA_i}}{D_{FFA_i}^{C_i} + r_{FFA_i} + D_{route}} \tag{16}$$

Whereby, r_{FFA_i} denotes the farthest distance between the center of FFA_i and its boundary, D_{route} represents the width of route. If the speed of aircraft V_R is higher than $V_{\max}^R$, then the aircraft will pass the crossover collision point first without causing any collision with the area. If its speed V_R is lower than $V_{\min}^R$, then the weather avoid field will pass the crossover collision point first without causing any collision with the aircraft; if the speed is within $\left[V_{\max}^R, V_{\min}^R\right]$, then there will be a collision.

3.1.2 Dynamic diversion steps

The steps of dynamic diversion route planning algorithm are:

(1) Based on expressions (15) and (16), decide whether there is a possibility of collision between the planned route with the weather avoid field. If so, go to step (2), otherwise the process ends;

(2) Locate the start and end points of the diversion and estimate the diversion time using expression (2). Use this time to compute the time slots n in the diversion segment. Calculate the corresponding location of weather avoid field at each time slot;

(3) Set the current time window $i=1$, for the corresponding location of the first time slot, using the static diversion route planning model and algorithm to generate a diversion route;

(4) $i=i+1$;

(5) Estimate the location of the aircraft with its speed and angle at the next time slot. If the distance between the two location is longer than 7.4km, using the current location as the start point of the diversion, and redo the static diversion route planning to get away from the corresponding weather avoid field of the *i*th time slot; otherwise, the last turning point is now the initial point of diversion, redo the static diversion route planning to get away from the corresponding weather avoid field of the *i*th time slot;

(6) If *i*=*n*, dynamic diversion route planning is completed, otherwise go to step (4).

4. CASE VERIFICATION

Taking Haikou-Nanjing Segment as an example, on the A470 route, between and GS, there are 3 weather avoid fields. When the weather avoid fields are generated, the distribution of those areas in a certain time window $\left[t_S, t_D\right]$ are as showed in Fig. 3. In this figure, the red polygon is the weather avoid field.

According to the distribution, take CJ as the starting point of the diversion, GS as the end point. After the transformation of coordinates, their coordinates are(46,54) and (0,0) respectively.

Based on the distance between CJ and GS, the estimated diversion time is 17 minutes (calculated by (2)). Therefore, the diversion would need to pass three time slots (1 slot = 6 minutes, the weather forecast interval). Fig.4 present the results of a prediction of the position and size of the weather avoid fields in the three time slots. In this Figure, the three red polygons from pale to dark are the weather avoid fields corresponding to the three time slots.

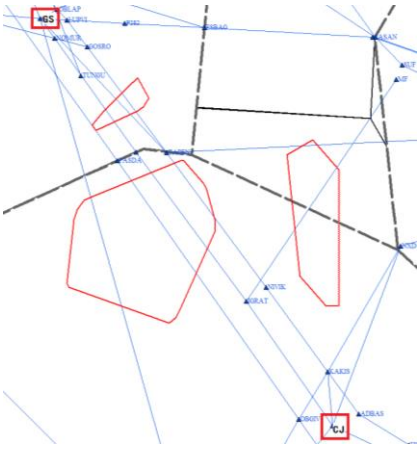

Figure 3 Distribution of weather avoid field in the Haikou-Nanjing Segment

From the Figure, it can be seen that area FFA1 is moving towards northwest and keeps expanding; FFA2 is moving towards southwest; and FFA3 is dissipating disappearing at the third time slot.

We use genetic-annealing algorithm to solve this problem. The parameters setting are as follows: size of initial population N=30, generation quantity G=10, initial temperature T_0=100, population crossover probability p_c=0.8, population mutation probability p_m=0.1, cooling coefficient q=0.8, ending temperature $Tend$=1. In the objective function, the weight coefficient of distance W_L=0.6, weight coefficient of diversion route safety ω_S=0.2, weight coefficient of the turning point ω_T=0.1, weight coefficient of turning angle ω_A=0.1, maximum turning points $N_{\max}$=8, allowable minimum safety value $R_S^{\min}=0.5$.

The static diversion route planning process is shown in Fig.5. The black solid line represents the original route, the blue dotted line represents the planned diversion route. The diversion route in Fig.5 is evaluated in terms of diversion distance, average diversion route safety, number of turning points and mean degrees of turning angles. The results are shown in table 2. The original route length between the start and end points of the diversion is 195km. The length of the planned diversion route is 215.15km, an increase of 10.3%. The average safety level of the diversion route is 0.8 with 1 turning point and a mean turning angle of 57.7 degrees.

The dynamic diversion route planning process is shown in Fig.6. The black solid line represents the original route. Point A is the location of the aircraft after the first time slot. Point B is the location after the second slot, while the blue dotted lines from pale to dark represent the three diversion planning routes begin with CJ, point A and point B respectively. The result dynamic diversion route is demonstrated in Fig.7. The blue dotted line is the final planned diversion route.

Table 3 presents the results of the evaluation of the dynamic diversion route. The length of the diversion is 198.38km, an increase of 1.7%.

Comparing the results of the dynamic and static diversion route planning methods, it can be seen that the route planned through dynamic diversion is safer, shorter and more operable.

Table 2 Evaluation results of static diversion route

Diversion distance	Average safety level	number of turning points	mean degrees of turning angles
215.15km	0.8	1	57.7°

Table 3 Evaluation results of static diversion route

Diversion distance	Average safety level	number of turning points	mean degrees of turning angles
198.38km	0.8	2	11.4°

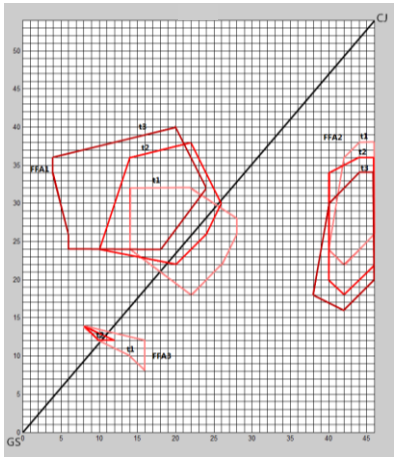

Figure 4 Demonstration of positions of weather avoid field

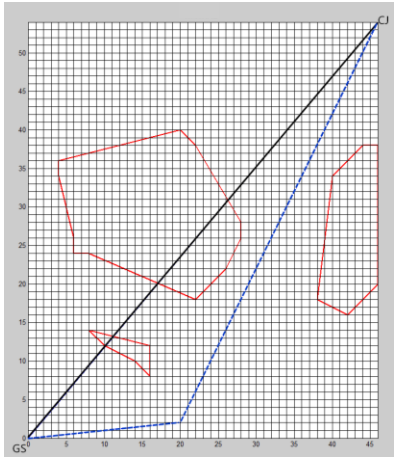

Figure 5 Result of genetic-annealing algorithm static diversion route planning

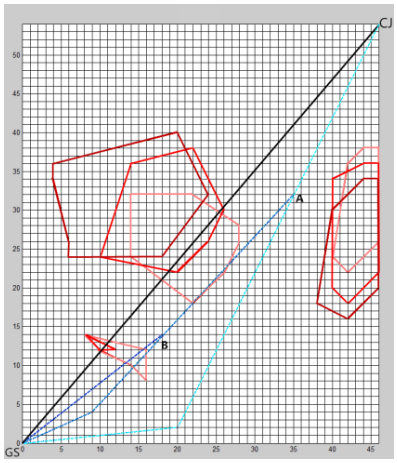

Figure 6 Dynamic route planning process

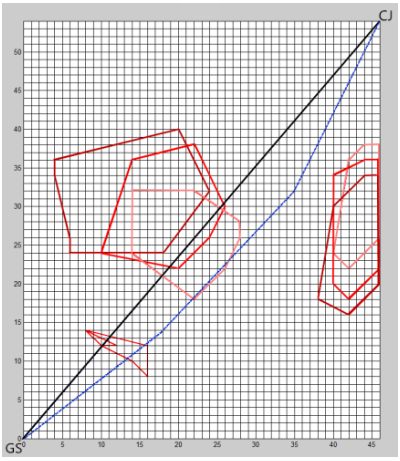

Figure 7 Demonstration of dynamic diversion route

5. CONCLUSION

The paper has studied the safety of diversion route required to avoid severe convective weather events. While sufficiently considering constraints such as pilot workload and aircraft performance, represented by number of turning points and mean turning angle. A dynamic diversion route planning mathematical model has been developed with a particular focus on safety, employing a genetic-annealing algorithm. The Haikou-Nanjing segment is used to verify the models. Simulation results have shown that the route planned through dynamic diversion is more economical and safety.

6. ACKNOWLEDGMENTS

We are grateful to CAAC Central and Southern Regional Administration for the provision of airspace structure data and weather data, and to the anonymous referees for valuable suggestions and comments.

7. REFERENCES

[1] Dixon M, Weiner G. “Automated aircraft routing through weather- impacted airspace”. IEEE International Conference on Robotics and Automation, Leuven, Belgium, 1998: 1725-1730.

[2] Song Ke. “The Research of Rerouting Problemin Air Traffie Flow Management. Nanjing University of aeronautics and astronautics,2002.

[3] Xu Xiaohao, Li Chenggong, Zhao Yifei, Li Xiong. “Rerouting path planning based on artificial potential field algorithm. Journal of Traffic and Transportation Engineering,2009,9(6): 64-68.

[4] Martin O.Nicholes, Chen-Nee Chuah, S.Felix Wu,,et al. “ Inter-domain collaborative routing (IDCR): Server selection for optimal client performance. Copmuter Communications 34(2011) 1798-1809.

[5] Taylor C, Wanke C. “Dynamically Generating Operationally Acceptable Route Alternatives Using Simulated Annealing. Air Traffic Control Quarterly, 2012, 20(1): 97.

[6] Paul F. Borchers, Keenan Roach, Louise Morgan-Ruszkowski. “Operational Evaluation of a Weather-Avoidance Rerouting System”. 14th AIAA Aviation Technology, Integration, and Operations Conference. AIAA 2014-2716.

[7] Chenfeng Xiong, Xiqun Chen, Xiang He, Xi Lin , Lei Zhang. “Agent-based en-route diversion: Dynamic behavioral responses and network performance represented by Macroscopic Fundamental Diagrams”. Transportation Research Part C 64 (2016) 148–163.

[8] Li Xiong. “Flight Rerouting Path Planning in Severe Weather. Nanjing University of aeronautics and astronautics, 2009.

8. COPYRIGHT